

Research Article

Deep Learning-Based Nonstationary Channel Prediction in Tactical Vehicle-to-Vehicle Communication Environments

Xin Lin ¹, Aijun Liu ¹, Chen Han,² Xiaohu Liang,³ Wenyu Wang ¹ and Enyu Li⁴

¹College of Communications Engineering in Army Engineering University of PLA, Nanjing 210000, China

²Sixty-Third Research Institute, National University of Defense Technology, Nanjing 21007, China

³School of Information Science and Engineering in Southeast University and the College of Communications Engineering in Army Engineering University of PLA, Nanjing 210000, China

⁴Department of Electronic Engineering of Qingdao University, Qingdao 266520, China

Correspondence should be addressed to Aijun Liu; liuj.cn@163.com

Received 11 May 2022; Revised 26 May 2022; Accepted 1 August 2022; Published 26 August 2022

Academic Editor: A.H. Alamooodi

Copyright © 2022 Xin Lin et al. This is an open access article distributed under the Creative Commons Attribution License, which permits unrestricted use, distribution, and reproduction in any medium, provided the original work is properly cited.

In this paper, we focus on the vehicle-to-vehicle dynamic channel in tactical communication environments, which shows time-varying and nonstationary characteristics due to the fast mobility, directional antennas, and harsh terrain. These situations present great challenges for the channel state information (CSI) acquisition. To obtain an accurate CSI and reduce pilot overhead, we propose a CSI predictor based on the long short-term memory (LSTM) network. As an improved recurrent neural network (RNN), LSTM units have an excellent learning result on both long- and short-term inputs by adding the gating mechanism. Using the outdated sampling CSI sequence as input data of LSTM units enables the predictor to extract complex data characteristics and capture the temporal law of the nonstationary channel. Simulation results are demonstrated to verify that the LSTM-based predictor has better performance than conventional algorithms in IEEE 802.11p standard. Additionally, the key factors that affect the performance of the proposed predictor are further analyzed.

1. Introduction

Tactical vehicle platforms include the armored vehicles and the unmanned ground vehicles (UGVs), which have been widely employed in the land battlefield nowadays [1]. These platforms are interconnected through the mobile ad hoc network (MANET) to perform the military missions [2]. In actual operations and maneuvers, the time-varying and nonstationary channel characteristics are caused by the fast mobility, directional antennas, and harsh terrain, which leads to poor transmission conditions and link interruption. Therefore, the reliability and validity of the vehicle-to-vehicle (V2V) wireless link are faced with great challenges. To tackle this problem, adaptive link transmission scheme and channel equalization techniques depending on the channel state information (CSI) are proposed to improve the system performance in this scenario [3–6]. Various data pilot-aided (DPA) channel estimation methods have been proposed to extract accurate CSI, which utilizes the

demapped data symbols as pilot information. The constructed data pilot (CDP) scheme evaluates the reliability of estimated subcarrier value by comparing the adjacent symbols and deciding whether or not to replace the estimated value [7]. The spectral temporal averaging (STA) algorithm [8] averages the estimated values in the time-frequency domain to reduce detection error. In test frequency domain interpolation (TRFI) scheme, the unreliable estimated value is renewed by frequency domain interpolation of the reliable data pilots [9]. However, these traditional DPA channel estimation approaches have difficulties in combating the dynamic time-frequency selective channel characteristics in such high mobile and complex environment [10]. On the one hand, the shorter coherence time and bandwidth will lead to frequent pilot insertion and reduce the effective communication rates [11]. On the other hand, the demapping and detection errors incur error propagation and limit the estimation performance. Additionally, estimated CSI will quickly be outdated due to the feedback

delay and nonstationary channel characteristics in the dynamic time-varying conditions [12].

Recently, deep learning (DL) techniques show great promise due to the powerful feature extraction capability and data-driven characteristics. Extensive research has applied DL techniques to DPA channel estimation process. The authors of [13] introduce an autoencoder- (AE-) based on neural network to conventional DPA channel estimation scheme where the AE is trained for updating the estimated value and attenuate the error propagation effect. In [14], the authors proposed a DL-based MIMO-OFDM channel estimation scheme. The convolutional neural network (CNN) and bidirectional long short-term memory (LSTM) are applied for frequency-domain interpolation and time-domain prediction, respectively. A gated recurrent unit- (GRU-) based channel estimation is developed in [15]. The error propagation in DPA process is suppressed by extracting the complex time-frequency correlation features. Simulation results show that the proposed method exhibits a performance gain without increasing computation complexity. In [16], a novel LSTM-based channel estimation scheme was designed for IEEE 802.11p standard in nonstationary V2V scenario. The proposed network structure is utilized for tracking channel characteristic and mitigating noise.

Compared with channel estimation techniques, channel prediction provides us with a more effective solution to the above problems. Based on the outdated historical CSI, channel prediction technique can extract the future CSI in a given period without sacrificing the scarce pilot resources and achievable data rates. Additionally, channel prediction technique can explore the changing law of the channel state and speculate on the future CSI in advance to weaken the effect of outdated information. Therefore, the channel prediction can overcome the disadvantage of excessive pilot overhead and outdated effect in channel estimation, which is suitable for the time-varying and nonstationary V2V channel. In this paper, we propose a predictor based on LSTM neural network for the dynamic V2V channel [17]. By introducing a new internal cell state and the gating mechanism, the LSTM neural network can not only record the history information but also control the path of data transmission. Therefore, the LSTM units are sensitive to both long- and short-term inputs. The LSTM-based predictor can capture the complex law of the dynamic channel and exploit the temporal correlation to get the accuracy and real-time CSI within a period. This method can not only avoid the extra pilot overhead but also improve the prediction accuracy by virtue of the powerful feature extraction capabilities of the LSTM neural network. The main contributions of our work are summarized as follows:

- (I) the system and V2V channel model in the tactical communication environments is developed, and the nonstationary channel characteristics are analyzed in detail.
- (II) To mitigate the effect of the outdated information, a two-stage LSTM-based prediction scheme is proposed to explore the temporal correlation of the CSI and realize the future CSI prediction.
- (III) The proposed predictor is shown to outperform the conventional algorithms by evaluating the normalized mean-squared error (NMSE) index. Besides, the impact of key factors on the propose scheme is analyzed in the end.

The remainder of this paper is organized as follows. Section 2 introduces the V2V system and nonstationary channel model for the tactical communication environments, in which the effect of fast mobility, directional antennas, and harsh terrain are taken into consideration. Section 3 proposes a two-stage LSTM-based channel prediction scheme and the architecture of the predictor. Simulation results that demonstrate the system performance are provided in Section 4. Finally, Section 5 gives the conclusions.

2. System and Nonstationary Channel Model

Figure 1 illustrates a point-to-point V2V communication system, where directional antennas are equipped in both transmit and receive platforms to improve the signal to interference plus noise ratio (SINR) and increase the communication distance in the tactical environments. Due to the complex scattering environment, the received signals can be divided into two components: the line-of-sight (LoS) component and the non-LoS (NLoS) component. Therefore, the channel impulse response can be expressed as

$$h(t, \tau) = \sqrt{\frac{K}{K+1}} h^{\text{LoS}}(t) \delta(\tau - \tau^{\text{LoS}}) + \sqrt{\frac{1}{K+1}} \sum_{n=1}^{N-1} h_n^{\text{NLoS}}(t) \delta(\tau - \tau_n^{\text{NLoS}}) \quad (1)$$

where K and N represent the Rice factor and the total number of the multipath component, respectively. $h^{\text{LoS}}(t)$ and τ^{LoS} represent the channel complex coefficient and the delay of the LoS component. $h_n^{\text{NLoS}}(t)$ and τ_n^{NLoS} are the channel complex coefficient and the delay of the n -th NLoS path. $h^{\text{LoS}}(t)$ and $h^{\text{NLoS}}(t)$ can be expressed as

$$h^{\text{LoS}}(t) = e^{j\phi^{\text{LoS}}} e^{j2\pi f_{D,Tx}^{\text{LoS}} \cos(\phi_{Tx}^{\text{LoS}} - \gamma_{Tx})t} \times e^{j2\pi f_{D,Rx}^{\text{LoS}} \cos(\phi_{Rx}^{\text{LoS}} - \gamma_{Rx})t}, \quad (2)$$

$$h_n^{\text{NLoS}}(t) = \sqrt{\frac{1}{N-1}} \lim_{M \rightarrow \infty} \frac{1}{\sqrt{M}} \sum_{m=1}^M e^{j\phi_m^{\text{NLoS},n}} \times e^{j2\pi f_{D,Tx}^{\text{NLoS},n} \cos(\phi_{Tx,m}^{\text{NLoS},n} - \gamma_{Tx})t} \times e^{j2\pi f_{D,Rx}^{\text{NLoS},n} \cos(\phi_{Rx,m}^{\text{NLoS},n} - \gamma_{Rx})t}, \quad (3)$$

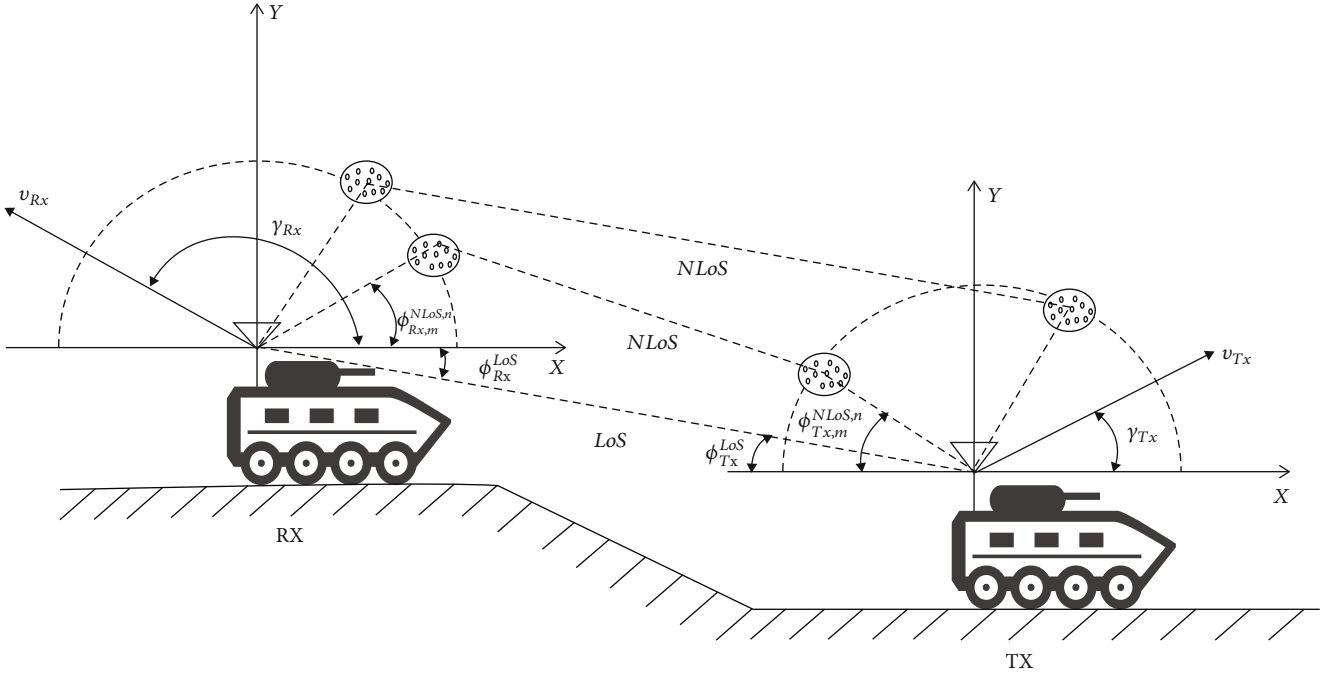


FIGURE 1: Point-to-point vehicle-to-vehicle communication system in the tactical environments.

where the channel variable $\{\Phi^{LoS}, f_{D,Tx}^{LoS}, f_{D,Rx}^{LoS}, \phi_{Tx}^{LoS}, \phi_{Rx}^{LoS}\}$ represents the initial phase, the maximal Doppler shift caused by the motion of TX, the maximal Doppler shift caused by the motion of RX, the direction of departure, and the direction of arrival of the LoS path, respectively. $\{\Phi_m^{NLoS,n}, f_{D,Tx}^{NLoS,n}, f_{D,Rx}^{NLoS,n}, \phi_{Tx,m}^{NLoS,n}, \phi_{Rx,m}^{NLoS,n}\}$ are the channel parameters of the m -th scattering path in the n -th NLoS path component. γ_{Tx} (γ_{Rx}) is the movement angle of the TX (RX) and M denotes the number of the scattered path. By taking the Fourier transform of Equation (1), the time-varying transmission function can be expressed as

$$H(t, f) = \int_{-\infty}^{+\infty} h(t, \tau) e^{-j2\pi f \tau} d\tau = \sqrt{\frac{K}{K+1}} h^{LoS}(t) e^{-j2\pi f \tau^{LoS}} + \sqrt{\frac{1}{K+1}} \sum_{n=1}^{N-1} h_n^{NLoS}(t) e^{-j2\pi f \tau_n^{NLoS}}. \quad (4)$$

Due to the fast mobility and low height of transmitting and receiving antennas deployed in mobile vehicle, the number and strength of propagation paths change frequently, so the channel statistic characteristics are time-varying, resulting in the nonstationary channel feature [11]. The “birth-death” process introduced in [18] is employed to model the “lifetime” of the multipath component, and the transi-

tion between “birth” and “death” can be described using the state transition matrix. In such tactical scenario, an additional term $z(t)$ can be used to account for the frequent changing state of the multipath component [19].

The directional antenna misalignment problem of the harsh terrains should be considered in the tactical environments. As shown in Figure 2, when mobile vehicle move on the flat terrain, the maximum gain direction of the transceiver antenna beam can be aligned. However, the main beam of the transceiver antenna cannot be aligned in the undulating terrain, resulting in a time-varying power loss of the propagation path. According to [20], the antenna power pattern $G(\theta, \psi)$ is applied to represent the directional misalignment effect, where $\{\theta, \psi\}$ denotes the direction of the antenna main beam. Based on the above analysis, the time-varying and nonstationary V2V channel in tactical communication environments can be reformulated as Equation (5), where the channel parameters $\{G(\theta_{Tx}^{LoS}, \psi_{Tx}^{LoS}), G(\theta_{Rx}^{LoS}, \psi_{Rx}^{LoS}), z^{LoS}(t)\}$ represent the directional antenna power pattern of TX and RX as well as the state of the LoS path, respectively. The channel parameters of the n -th path in the NLoS component are $\{G(\theta_{Tx,n}^{NLoS}, \psi_{Tx,n}^{NLoS}), G(\theta_{Rx,n}^{NLoS}, \psi_{Rx,n}^{NLoS}), z_n^{NLoS}(t)\}$. Note that the propagation environment changes during the moving process; thus, the parameters in Equation (5) are all time-varying.

$$H(t, f) = \sqrt{\frac{K}{K+1}} \sqrt{G(\theta_{Tx}^{LoS}, \psi_{Tx}^{LoS}) G(\theta_{Rx}^{LoS}, \psi_{Rx}^{LoS})} z^{LoS}(t) h^{LoS}(t) e^{-j2\pi f \tau^{LoS}} + \sqrt{\frac{1}{K+1}} \sum_{n=1}^{N-1} \sqrt{G(\theta_{Tx,n}^{NLoS}, \psi_{Tx,n}^{NLoS}) G(\theta_{Rx,n}^{NLoS}, \psi_{Rx,n}^{NLoS})} z_n^{NLoS}(t) h_n^{NLoS}(t) e^{-j2\pi f \tau_n^{NLoS}}. \quad (5)$$

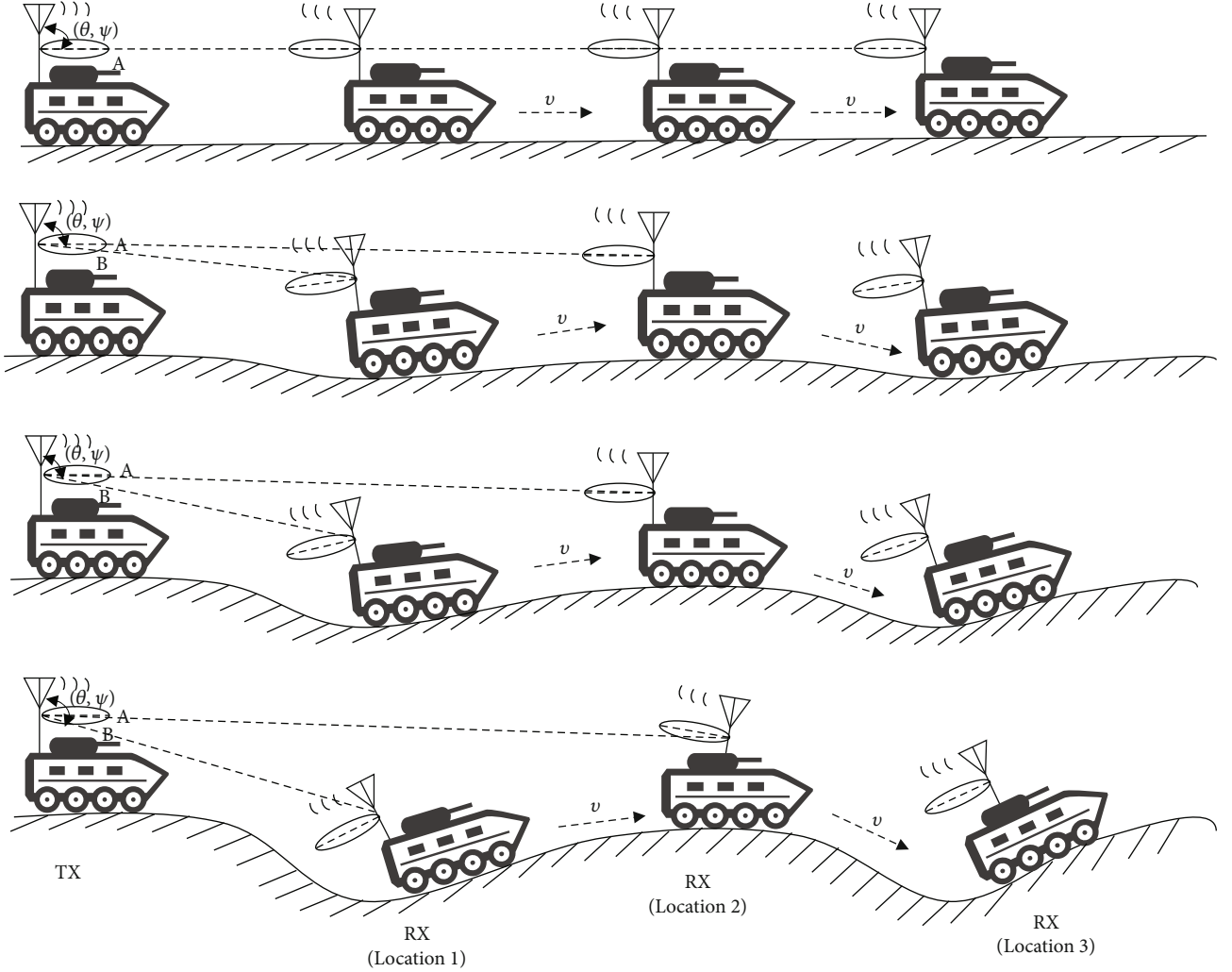


FIGURE 2: The misaligned angle of the transceiver antenna in different terrains.

3. Long Short-Term Memory-Based Channel Prediction

According to the above analysis, the CSI obtained using the channel estimation technique is outdated due to the significant time-varying and nonstationary channel characteristics. Here, we employ an LSTM-based predictor to explore complex channel characteristics and extract real-time CSI. The proposed model is trained and optimized by minimizing the root mean square error (RMSE) $J(\Theta)$ between the predicted CSI $\hat{H}(t, f)$ and supervision value $H(t, f)$. $J(\Theta)$ can be expressed as \hat{A}

$$J(\Theta) = \sqrt{\frac{1}{Q} \sum_{q=1}^Q [\hat{H}_q(t, f) - H_q(t, f)]^2}, \quad (6)$$

where Q denotes the number of channel sequence samples in the training process.

3.1. Two-Stage Prediction Scheme. The whole prediction scheme can be divided into two stages: the training and prediction stage, as shown in Figure 3.

The proposed LSTM-based predictor will learn the correlation between the historical CSI in the training stage. Then, the trained model takes the outdated CSI as the input data to extract the future moment CSI in the prediction stage. Note that the training stage is complex and time-consuming, but it can be finished in offline mode. Moreover, with the development of hardware technology, high-performance processing modules are deployed in tactical devices. Hence, the computing power and processing capacity of tactical devices has been greatly enhanced, which can support the computational requirement of the proposed approach.

3.2. Architecture of the Channel Predictor. Figure 4 illustrates the architecture of the proposed LSTM-based channel predictor. By adding the cell state and the gating mechanism, the LSTM cell addresses the problem of gradient explosion or disappearance of the RNN. The LSTM cell is mainly

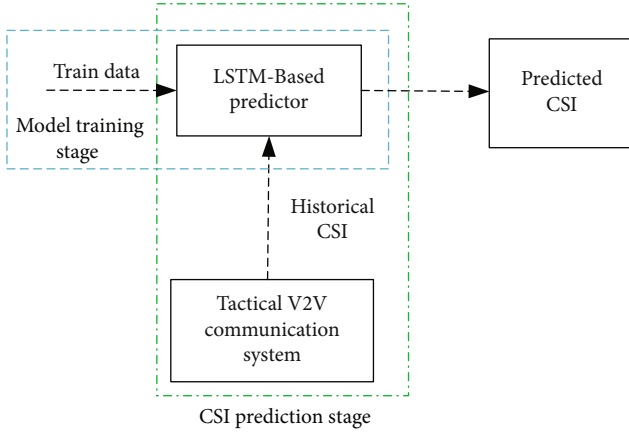


FIGURE 3: Two-stage prediction scheme for vehicle-to-vehicle channel in tactical communication environment.

composed of three gates, namely, the forget gate f_t , the input gate i_t , and the output gate o_t . The three gates and candidate states \tilde{c}_t are calculated by the external state h_{t-1} at the previous moment and the input $x_t \in \mathbb{R}^{M \times 1}$, which can be expressed as

$$f_t = \sigma(W_f \cdot [x_t, h_{t-1}] + b_f), \quad (7)$$

$$i_t = \sigma(W_i \cdot [x_t, h_{t-1}] + b_i), \quad (8)$$

$$o_t = \sigma(W_o \cdot [x_t, h_{t-1}] + b_o), \quad (9)$$

$$\tilde{c}(t) = \tanh(W_c \cdot [x_t, h_{t-1}] + b_c), \quad (10)$$

where $\{W_f, W_i, W_o, W_c\}$ and $\{b_f, b_i, b_o, b_c\}$ are weight matrices and bias vectors for LSTM units, respectively. The gates f_t and i_t are then combined to update the memory unit c_t , as shown in Equation (11) and Equation (12). Finally, by calculating c_t and o_t , the internal state is transferred to the next external state h_t .

$$c_t = f_t \odot c_{t-1} + i_t \odot \tilde{c}_t, \quad (11)$$

$$h_t = o_t \odot \tanh(c_t). \quad (12)$$

The above process can not only achieve the linear transmission of the cyclic information but also nonlinearly output the information to the external state. Therefore, the LSTM neural network can realize excellent learning results for time series in both long and short terms. During the training process, the LSTM structure will automatically learn and update the weight matrix W_* and bias term b_* . The LSTM Layer1 is an input layer to receive historical CSI, and the two following LSTM layers play a key role in exploring the temporal features of the nonstationary channel. Finally, the output layer is a fully connected layer, which will reshape and output the predicted CSI $\hat{H}(t, f)$. The rectified linear unit (Relu) function is selected as the activate function for all layers. It should be noted that the neural network modules are only

capable of dealing with the real-valued data, but channel coefficients are complex-valued. To improve the efficiency, most articles decompose complex channel coefficients into real and imaginary parts in training stage [13, 15, 16]. In test stage, the separating parts predicted by the neural network will be recombined into the complex value as the channel coefficients. The LSTM-based V2V channel prediction algorithm for tactical communication environments can be summarized as Algorithm 1.

3.3. Computation Complexity Analysis. In this subsection, the multiply accumulate (MAC) operation is used to analyze the computation complexity of the proposed LSTM-based predictor, which comes from the matrix operation of the neural network. The CSI sample $x_t \in \mathbb{R}^{M \times 1}$ is the input data of the LSTM Layer1, whose weight matrices and bias vectors are $W_i, W_o, W_f, W_c \in \mathbb{R}^{(M+L_1) \times L_1}$ and $b_i, b_o, b_f, b_c \in \mathbb{R}^{L_1 \times 1}$, respectively. Therefore, the MAC operation for the first LSTM layer is $4K[(M+L_1)L_1 + L_1]$ where K is the length of the input sequence. For the other LSTM layers ($2 \leq j \leq J$), the input data is $h_{t-1} \in \mathbb{R}^{(L_{j-1} \times 1)}$, so the MAC operation for them is $4K \cdot [\sum_{j=2}^J (2L_{j-1} \cdot L_j + L_j)]$. Finally, MAC operation for the output layer can be expressed as $4K \cdot (L_j \cdot M + M)$.

4. Numerical Simulation Result

In this section, simulation results are performed to validate the performance of the proposed prediction scheme. The simulations are performed on the TensorFlow-GPU 2.0.0 platform and relevant parameters are set as follows. The total number of paths is set to 12 and the Rician factor K is 20 dB. The amplitude of the multipath component follows Rayleigh distribution. For the directional antennas, a half-wave oscillator antenna is selected, whose maximum beam angle is 78° . The neuron numbers in the three LSTM layers are 128, 256, and 512, respectively. To avoid overfitting, we set the dropout value to 0.3. To improve the training efficiency, the Adam optimizer is used. The epoch limit for training and the batch size are 500 and 128, respectively. The sizes of training and test sets are 20000 and 2000, respectively. To verify the generalization property of the proposed algorithm, the channel model parameters of test set are not the same as the training one. There are new channel parameters for the test set. For example, the test set included terrain and Doppler shift parameters that were not presented in training set. In addition, the channel prediction is performed based on the outdated CSI, which will be regarded as the input data for neural network model. In this paper, we adopt the traditional comb-type pilot pattern to estimate the outdated CSI. The pilot symbols are equally distributed on the subcarriers with a spacing of 4. The length of input sequence is set to 30. Absolutely, as the input length increases, more channel features can be captured by LSTM networks, and the changing law of channel can be extracted more accurately. Certainly, as the dimension of input data increases, the complexity of neural networks also increases greatly.

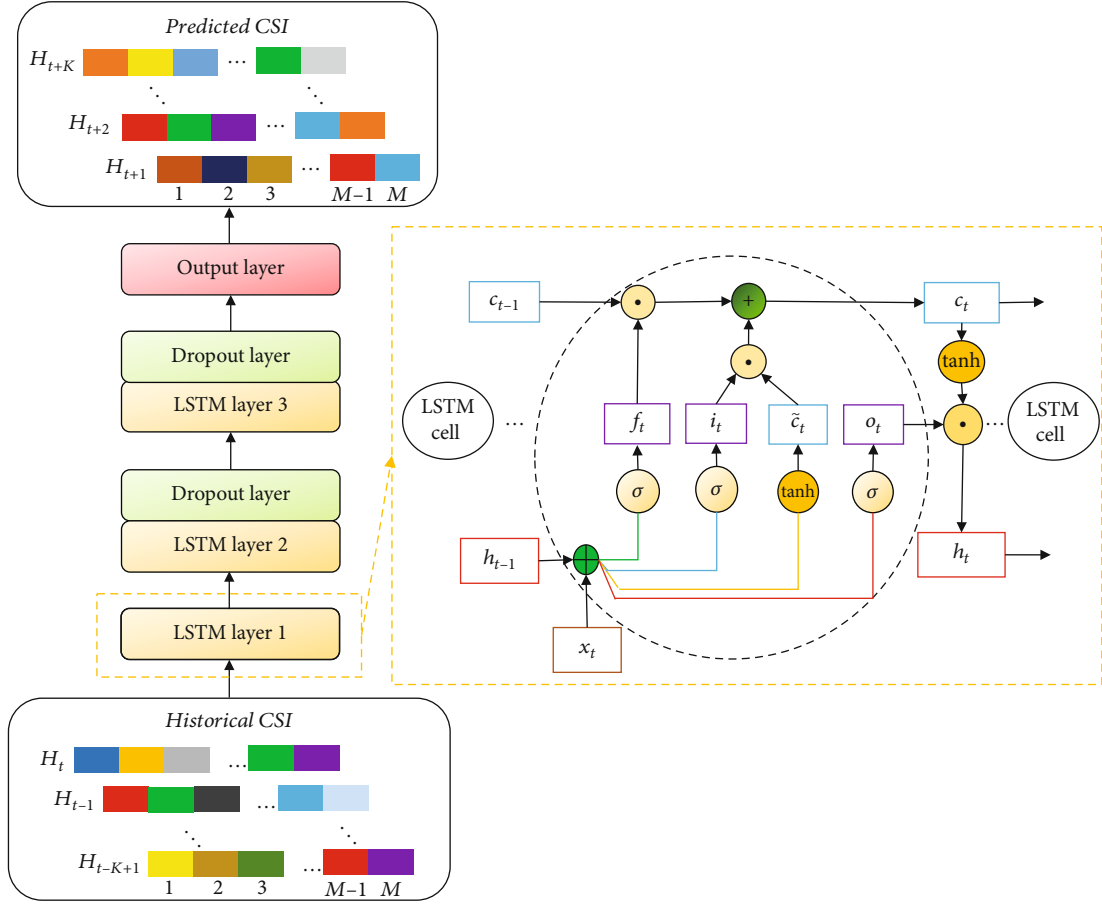


FIGURE 4: The architecture of the long short-term memory-based prediction framework.

input: Complex CSI sequence, the set of hyperparameters Θ .

1: **Training stage:**

2: Generate the input data of the training set by dividing the complex channel sequence into two subsequences according to the real and imaginary component.

3: **for** epoch $e = 1 : E$ **do**

4: Explore the temporal non-stationary characteristics of the V2V channel using the LSTM-based neural networks model.

5: Obtain the predicted CSI via the model.

6: The hyperparameters are optimized by minimizing the loss function $J(\Theta)$ in Equation (6).

7: **end**

8: **Prediction stage:**

9: Generate the test input data by converting the complex data to real domain.

10: Predict the target CSI via inputting the historical data into the trained LSTM-based predictor.

output: The trained LSTM-based channel predictor.

ALGORITHM 1: The long short-term memory-based vehicle-to-vehicle channel prediction algorithm for tactical communication environments.

To evaluate the prediction accuracy, we take the normalized mean square error (NMSE) as the performance index, which can be calculated using

$$\text{NMSE} = E \left\{ \frac{1}{P} \sum_{p=1}^P \frac{\|\hat{H}_p(t, f) - H_p(t, f)\|_2^2}{\|H_p(t, f)\|_2^2} \right\}, \quad (13)$$

where P is the total number of the test samples and $E\{\cdot\}$ denotes the expectation operation.

We first analyze the temporal correlation of the V2V channel with different Doppler shift, as shown in Figure 5(a). As the Doppler shift decreases, the correlation coefficient gradually increases due to the longer coherence time, indicating that the channel information is predictable within a certain time interval. Figure 5(b) shows the

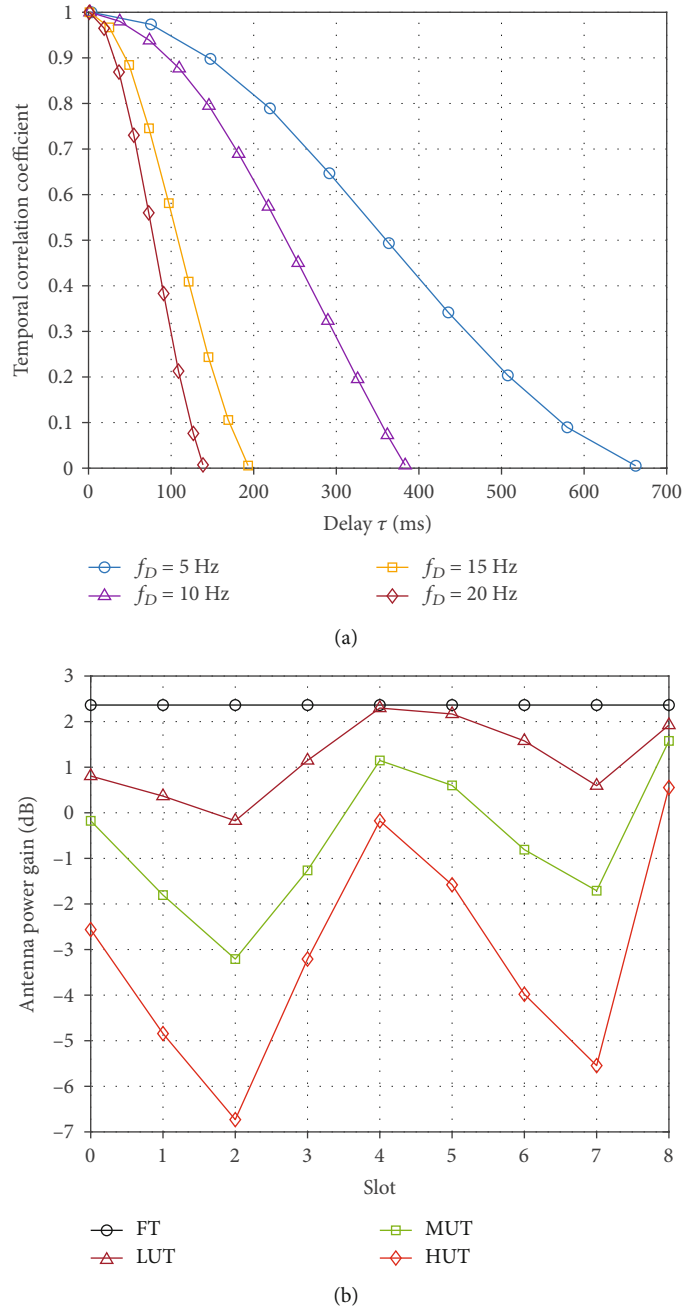


FIGURE 5: (a) Temporal correlation characteristic with different maximal Doppler shifts. (b) Comparison of the antenna power gain in different terrain conditions.

comparison results of antenna pattern gain in four terrain conditions, including flat terrain (FT), lightly undulating terrain (LUT), moderately undulating terrain (MUT), and heavily undulating terrain (HUT). It can be seen that a more undulating terrain will cause severe fluctuations of directional antenna gain and make the changing law of the V2V channel more complex, which will bring more challenges to channel prediction.

As shown in Figure 6, the conventional channel estimation algorithms in IEEE 802.11p standard, such as con-

structed data pilots (CDP) [7] and spectral temporal averaging (STA) [8], show bad performance due to the estimation error propagation effect caused by noise and channel variation. Compared with conventional algorithms, the proposed LSTM-based predictor realizes performance improvement due to the strong ability of the DNNs in extracting complex features and correlation relationships. For a fair comparison, the multilayer perceptron (MLP) in [21] is deployed with the same number of layers and neurons as the proposed LSTM-based predictor. Due to the great

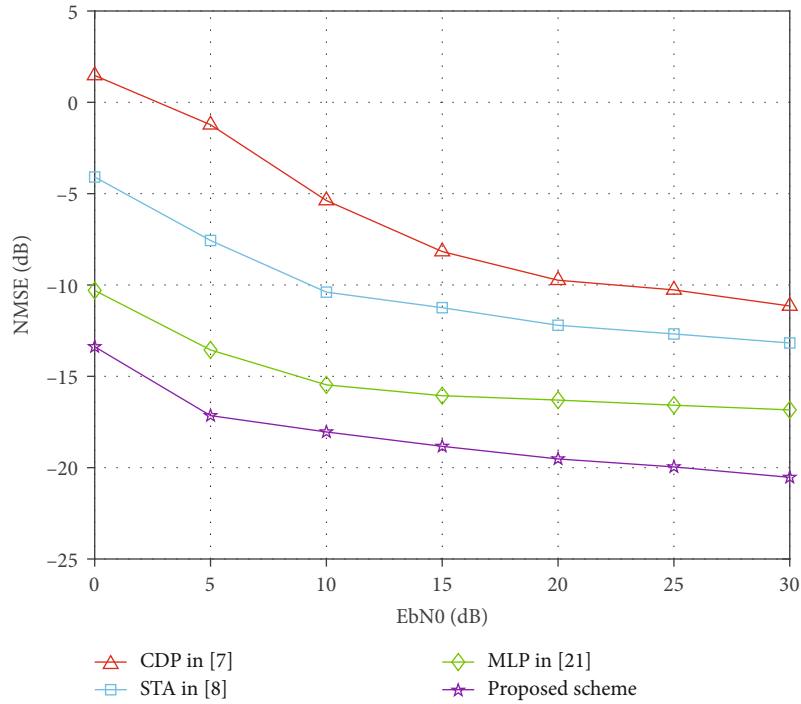


FIGURE 6: The NMSE of the proposed scheme and conventional algorithms for different SNRs.

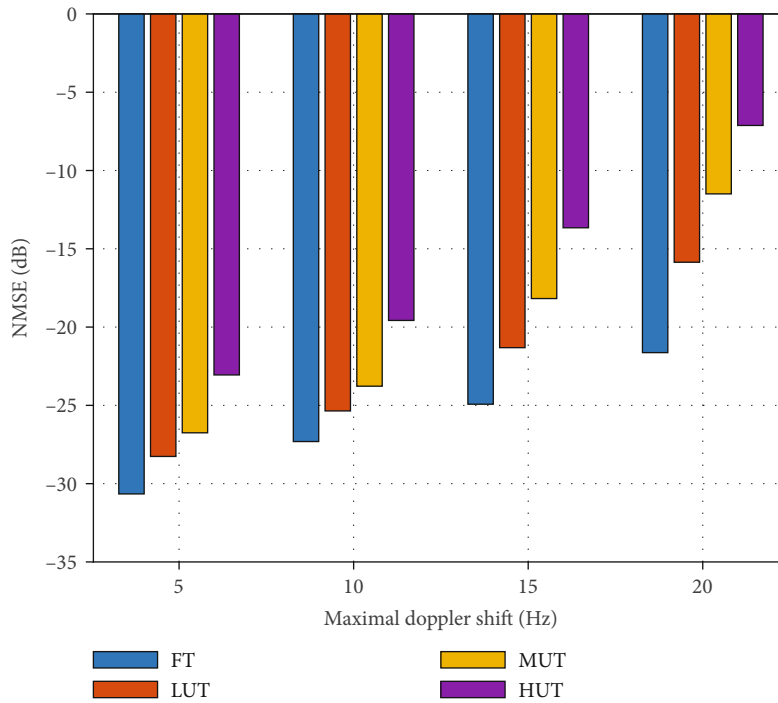


FIGURE 7: The NMSE of the proposed scheme for different terrain with different vehicle speeds.

advantages of the LSTM neural networks in processing time-series data, there is also a performance gain between the proposed scheme and MLP.

Figure 7 analyzes the key factors that affect the performance of the proposed scheme. The training and test data-

sets of the four terrains are generated according to the direction of antennas main lobe $\{\theta, \psi\}$ in corresponding terrains. The mobility scenarios are indicated by the maximal Doppler shift of 5, 10, 15, and 20 Hz, which are consistent with the vehicle speed. Therefore, the training and test

datasets of different Doppler shift are generated according to different vehicle speed in actual scenario. With the increase in the Doppler shifts, the temporal correlation of the V2V channel weakens and the prediction accuracy gradually decreases. Additionally, it is intuitive that the proposed scheme is more suitable to be applied for the less undulating terrain under the same vehicle speed. This is because the temporal changing law of antenna gain is more complex in undulating terrain, which will increase the difficulty for the LSTM-based model to extract the channel characteristics and reduce the accuracy of the performance.

5. Conclusion

In this paper, we first introduced the V2V channel model and nonstationary characteristic in tactical communication environments. Then, we proposed a LSTM-based channel predictor to reduce pilot overhead and mitigate the impacts of outdated information. The simulation results showed that the proposed method can get better prediction accuracy than other conventional algorithms in the index of NMSE. Based on above analysis, it can be concluded that the terrain conditions and the vehicle speed influence on the performance of the proposed scheme. In future work, we will design the adaptive transmission scheme according to the predicted CSI to overcome the adverse influence of the V2V channel and improve the reliability and validity of the tactical communication system.

Data Availability

The original data used to support this work is generated by MATLAB 2019, and the method of dataset generation is included within the manuscript.

Conflicts of Interest

The authors declare that they have no conflicts of interest.

Acknowledgments

This work was supported in part by the National Key Research and Development Program of China under Grant 2018YFB1801103, in part by the Natural Science Foundation on Frontier Leading Technology Basic Research Project of Jiangsu Province under Grant BK20192002, in part by the National Natural Science Foundation of China under Grant 61901516, in part by the China Postdoctoral Science Foundation under Grant 2019M651648, and in part by the Natural Science Foundation of Jiangsu Province under Grant BK20180578.

References

- [1] J. S. Lee, Y.-S. Yoo, H. S. Choi, T. Kim, and J. K. Choi, "Energy-efficient TDMA scheduling for UVS tactical MANET," *IEEE Communications Letters*, vol. 23, no. 11, pp. 2126–2129, 2019.
- [2] B. Roh, M. H. Han, M. Hoh, K. Kim, and B. H. Roh, "Tactical MANET architecture for unmanned autonomous maneuver network," in *MILCOM 2016-2016 IEEE Military Communications Conference*, pp. 829–834, Baltimore, MD, USA, 2016.
- [3] A. Duel-Hallen, "Fading channel prediction for mobile radio adaptive transmission systems," *Proceedings of the IEEE*, vol. 95, no. 12, pp. 2299–2313, 2007.
- [4] W. Jiang and H. D. Schotten, "Deep learning for fading channel prediction," *IEEE Open Journal of the Communications Society*, vol. 1, pp. 320–332, 2020.
- [5] M. Wen, B. Ye, E. Basar, Q. Li, and F. Ji, "Enhanced orthogonal frequency division multiplexing with index modulation," *IEEE Transactions on Wireless Communications*, vol. 16, no. 7, pp. 4786–4801, 2017.
- [6] J. Li, S. Dang, Y. Yan, Y. Peng, S. Al-Rubaye, and A. Tsourdos, "Generalized quadrature spatial modulation and its application to vehicular networks with NOMA," *IEEE Transactions on Intelligent Transportation Systems*, vol. 22, no. 7, pp. 4030–4039, 2021.
- [7] J. A. Fernandez, K. Borries, L. Cheng, B. V. K. Vijaya Kumar, D. D. Stancil, and F. Bai, "Performance of the 802.11p physical layer in vehicle-to-vehicle environments," *IEEE Transactions on Vehicular Technology*, vol. 61, no. 1, pp. 3–14, 2012.
- [8] Z. Zhao, X. Cheng, M. Wen, B. Jiao, and C.-X. Wang, "Channel estimation schemes for IEEE 802.11p standard," *IEEE Intelligent Transportation Systems Magazine*, vol. 5, no. 4, pp. 38–49, 2013.
- [9] Y.-K. Kim, J.-M. Oh, Y.-H. Shin, and C. Mun, "Time and frequency domain channel estimation scheme for IEEE 802.11p," in *17th International IEEE Conference on Intelligent Transportation Systems (ITSC)*, pp. 1085–1090, Qingdao, China, 2014.
- [10] X. Lyu, W. Feng, N. Ge, and X. Wang, "Deep learning-based symbol detection for time-varying nonstationary channels," *China Communications*, vol. 19, no. 3, pp. 158–171, 2022.
- [11] R. M. Rao, V. Marojevic, and J. H. Reed, "Adaptive pilot patterns for CA-OFDM systems in nonstationary wireless channels," *IEEE Transactions on Vehicular Technology*, vol. 67, no. 2, pp. 1231–1244, 2018.
- [12] W. Jiang and H. D. Schotten, "Neural network-based fading channel prediction: a comprehensive overview," *IEEE Access*, vol. 7, pp. 118112–118124, 2019.
- [13] S. Han, Y. Oh, and C. Song, "A deep learning based channel estimation scheme for IEEE 802.11p systems," in *ICC 2019-2019 IEEE International Conference on Communications (ICC)*, pp. 1–6, Shanghai, China, 2019.
- [14] Y. Liao, Y. Hua, and Y. Cai, "Deep learning based channel estimation algorithm for fast time-varying MIMO-OFDM systems," *IEEE Communications Letters*, vol. 24, no. 3, pp. 572–576, 2020.
- [15] J. Hou, H. Liu, Y. Zhang, W. Wang, and J. Wang, "GRU-based deep learning channel estimation scheme for the IEEE 802.11p standard," *IEEE Wireless Communications Letters*, 2022.
- [16] J. Pan, H. Shan, R. Li, Y. Wu, W. Wu, and T. Q. S. Quek, "Channel estimation based on deep learning in vehicle-to-everything environments," *IEEE Communications Letters*, vol. 25, no. 6, pp. 1891–1895, 2021.
- [17] C. Luo, J. Ji, Q. Wang, X. Chen, and P. Li, "Channel state information prediction for 5G wireless communications: a deep learning approach," *IEEE Transactions on Network Science and Engineering*, vol. 7, no. 1, pp. 227–236, 2020.
- [18] C. Li, L. Liu, and J. Xie, "Finite-state Markov wireless channel modeling for railway tunnel environments," *China Communications*, vol. 17, no. 2, pp. 30–39, 2020.

- [19] I. Sen and D. W. Matolak, "Vehicle-vehicle channel models for the 5-GHz band," *IEEE Transactions on Intelligent Transportation Systems*, vol. 9, no. 2, pp. 235-245, 2008.
- [20] H. Yang, M. H. A. J. Herben, I. J. A. G. Akkermans, and P. F. M. Smulders, "Impact analysis of directional antennas and multiantenna beamformers on radio transmission," *IEEE Transactions on Vehicular Technology*, vol. 57, no. 3, pp. 1695-1707, 2008.
- [21] A. K. Gizzini, M. Chafii, A. Nimr, and G. Fettweis, "Deep learning based channel estimation schemes for IEEE 802.11p standard," *IEEE Access*, vol. 8, pp. 113751-113765, 2020.